Comments

Comments are short papers which comment on papers of other authors previously published in the **Physical Review**. Each Comment should state clearly to which paper it refers and must be accompanied by a brief abstract. The same publication schedule as for regular articles is followed, and page proofs are sent to authors.

Noise effect on instabilities and chaotic solutions of a superconducting interferometer

R. Leoni, P. Carelli, and V. Foglietti

Istituto di Elettronica dello Stato Solido del Consiglio Nazionale delle Ricerche,
Via Cineto Romano 42, 00156 Roma, Italy

(Received 7 February 1986)

A computer simulation of a dc superconducting quantum interference device (dc SQUID) in the case $\beta_c = 3$, $\beta_L = 6.28$, and noise parameter $\Gamma = 0.01$ is performed. The main difference with respect to the case of noiseless behavior is the disappearing and/or mixing of some solutions of the differential equations describing the time evolution of the system. Only by including the noise effect in the simulation is it possible to understand the working mechanism of some practical devices characterized by high values of the critical current and inductance.

The relatively simple system made up of two Josephson junctions connected in a superconducting loop, usually called the dc superconducting quantum interference device (dc SQUID), has been widely studied numerically. The first attempt to solve the problem was made by neglecting the junction capacitance.[1] The inclusion of the capacitance term[2] showed that the optimum performances were similar to those obtained in the first calculation. More recently, it has been shown[3] that when particular values of the parameters controlling the dynamics of the system are chosen the dc SQUID behavior becomes very complicated and the solutions of the differential equations describing the system become chaotic. In this case, the relevant characteristics of the device dramatically degrade so much as to prevent its use as a magnetometer.

In this Comment we investigate what happens to this kind of solution when the dynamics of the system is perturbed by the noise related to the dissipative part of the dc SQUID, numerically solving the two second-order differential equations governing the system's time evolution. We show that here the noise plays an important role and can change the relevant characteristics of the SQUID a lot, probably more than in the case usually considered in the design of superconducting magnetometers.

The resistively-shunted-junction model of a Josephson junction in the symmetrical case permits one to write[2]

$$I_i = (\phi_0 C/2\pi)d^2\delta_i/d^2 t + (\phi_0/2\pi R)d\,\delta_i/dt$$

$$+ I_c \sin\delta_i + I_{ni} \quad \text{for } i = 1,2 , \tag{1}$$

where δ_i is the phase difference, C is the junction capacitance, R is the shunt resistance, I_c is the junction critical current, I_{ni} is the noise current, and ϕ_0 is the flux quantum. Using flux quantization and following Ref. 3 the dimen-

sionless equations can be written

$$\beta_c \ddot{v} + \dot{v} + \sin v \cos\theta = i/2 - (i_{n1} + i_{n2})/2, \tag{2a}$$

$$\beta_c \ddot{\theta} + \dot{\theta} + \sin\theta \cos v + 2\theta/\beta_L = \theta_{\text{ext}}/\beta_L - (i_{n1} - i_{n2})/2 , \tag{2b}$$

where $\beta_c = 2\pi R^2 C I_c/\phi_0$, $\beta_L = 2\pi L I_c/\phi_0$, $\theta_{\text{ext}} = 2\pi\phi_{\text{ext}}/\phi_0$, ϕ_{ext} is the external magnetic flux coupled to the dc SQUID, $i = (I_1 + I_2)/I_c$, and $i_{ni} = I_{ni}/I_c$. Furthermore, $v = (\delta_1 + \delta_2)/2$ is the average phase difference and $\theta = (\delta_1 - \delta_2)/2$ is the internal phase difference. Dotted variables represent derivatives with respect to the reduced time $t' = t 2\pi I_c R/\phi_0$. In this scheme the voltage V which appears at the terminals of the dc SQUID is $\dot{v}RI_c$ and the circulating current J (in units of I_c) flowing inside the superconducting loop is related to the internal phase by

$$J = (I_1 - I_2)/2I_c = 2(\theta - \theta_{\text{ext}}/2)/\beta_L . \tag{3}$$

We assume that the noise currents i_{n1} and i_{n2} arise from the Johnson noise generator in the shunt resistances, so that in this low-frequency approximation each one has a white spectral density $S_I = 4k_B T/R$ where k_B is Boltzmann's constant. Applying the time transformation in reduced units we can write

$$S_i = (4k_B T/R)(1/I_c)^2(2\pi I_c R/\phi_0) = 4\Gamma , \tag{4}$$

where $\Gamma = 2\pi k_B T/I_c\phi_0$ is the noise parameter.

From Eq. (2) it is clear that the effect of noise is to change randomly the working point of the dc SQUID defined by i and θ_{ext}. Furthermore, as is well known, these equations show that the problem of understanding the dc SQUID behavior can be reduced to the more intuitive study of the dynamics of a classical particle having mass β_c, placed in the position defined by the coordinates v and θ, moving in a bidimensional potential given by

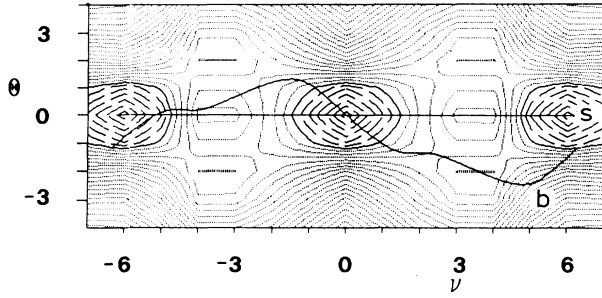$$U(v,\theta) = -\cos v \cos\theta + \theta^2/\beta_L , \tag{5}$$

FIG. 1. Isopotential contour plot in the (v,θ) plane in the case $\beta_L = 6.28$. The trajectories labeled s and b represent two possible solutions of Eq. (2) in the case $\beta_c = 3$, $i = 1.5$, $\theta_{ext} = 0$, and $\Gamma = 0$.

and subject to a force of components in the v and θ directions given by

$$i_v = i/2 - (i_{n1} + i_{n2})/2 \,, \tag{6a}$$

$$i_\theta = \theta_{ext}/\beta_L - (i_{n1} - i_{n2})/2 \,, \tag{6b}$$

respectively.

In Fig. 1 the isopotential contour plot in the case $\beta_L = 6.28$ is shown. In this figure two possible trajectories of the particle in the case $\beta_c = 3$, $i = 1.5$, $\theta_{ext} = 0$, and $\Gamma = 0$ are also indicated.

Assuming $\theta_{ext} = 0$ the possible solutions of Eq. (2) fall in one of the following categories.[3]

(1) They could fall into a zero-voltage state in which the particle is confined in the proximity of one of the absolute minima of the potential. In contrast to the other kind of solutions this is a static solution (i.e., $\dot{v} = \dot{\theta} = 0$).

(2) They might fall into a single-junction state (trajectory s in Fig. 1) in which $\theta = 0$ and $\dot{v} \neq 0$. The potential $U(v,0)$ is the same as in the case of the single Josephson junction.

(3) Or they could fall into a beating state (trajectory b in Fig. 1) with $\theta \neq 0$ and $\dot{v} \neq 0$, whose characteristic frequency is governed, as discussed in Ref. 4, by the LC circuit. The beating solution exists only for a limited range of values β_L and β_c. This solution is characterized by low average voltage and high rms values of the circulating current.

The i-$\langle \dot{v} \rangle$ characteristics of the dc SQUID without noise in the case of $\beta_L = 6.28$ and $\beta_c = 3$ are shown in Figs. 2(a), 2(b), and 2(c) for values of θ_{ext} equal to 0, 0.7, and 1.57, respectively. The zero-voltage and single-junction branches were obtained starting from $i = 0$ and initial conditions $v_0 = \theta_0 = \dot{v}_0 = \dot{\theta}_0 = 0$ (i.e., a particle at rest in an absolute minimum of Fig. 1), and computing $\langle \dot{v} \rangle$ on the basis of the numerically calculated solutions of Eq. (2). Next, the current i is slightly increased and a new computation is performed, taking as initial conditions for the four variables the last temporal values obtained in the previous calculation. The average is always performed in the steady-state condition. This procedure is repeated until a given maximum value of the bias current i is reached; from this point we go back decreasing the current i. The beating branch, that in this case coexists with other ones, is searched by always placing the particle at $t = 0$ in the
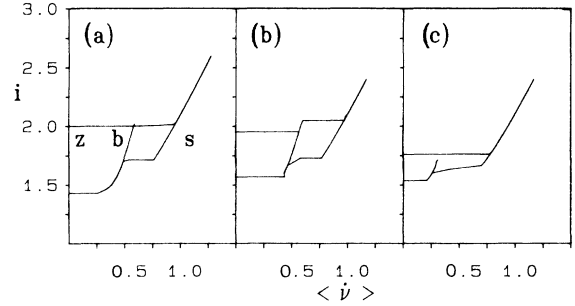

FIG. 2. i-$\langle \dot{v} \rangle$ characteristics in the case $\beta_L = 6.28$, $\beta_c = 3$, and $\Gamma = 0$ in correspondence of (a) $\theta_{ext} = 0$, (b) 0.7, and (c) 1.57. Labels z, b, and s indentify the zero voltage branch, the beating branch, and the single junction branch, respectively.

proximity of a secondary minimum of the potential and giving it an initial velocity only in the θ direction (i.e., $v_0 = 3.14$, $\theta_0 = 3$, $\dot{v}_0 = 0$, and $\dot{\theta}_0 = 1$). All the solutions of the second-order differential equations were numerically calculated using the Milne's method.[5]

The case studied in Fig. 2(a) is the same as in Ref. 3. The agreement is quite good. [Note that the current normalization is different. Here $i = (I_1 + I_2)/I_c$, in Ref. 3 $i = (I_1 + I_2)/2I_c$.] Note the abrupt displacement of the beating branch into the low-voltage region on moving from Fig. 2(b) to Fig. 2(c). The names of the three branches, defined in the case $\theta_{ext} = 0$ [Fig. 2(a)], are used to label similar solutions in the other cases discussed ($\theta_{ext} \neq 0$).

In order to gain more insight about the dc SQUID features as a magnetometer in this parameter range, the average voltage versus the external flux was computed in the absence of noise in the case $\beta_L = 6.28$ and $\beta_c = 3$. In Fig. 3 the curves at $i = 1.6$ and $i = 1.8$ are shown. The agreement between the curve corresponding to $i = 1.6$ and Fig. 7(a) of Ref. 3 seems to be very good. At $i = 1.6$, $\theta_{ext} = 0.8$ or 5.5, the solution of the SQUID equations is chaotic. This solution is reached via a Feigenbaum sequence. The almost flat flux dependence of $\langle \dot{v} \rangle$ seems to prevent the use of such a device as a magnetic field detector.

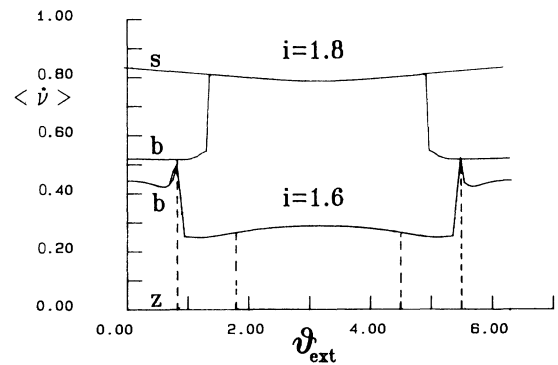Nevertheless there are in the literature experimental

FIG. 3. $\langle \dot{v} \rangle$-θ_{ext} characteristics corresponding to the current $i = 1.6$ and 1.8 in the case $\beta_L = 6.28$, $\beta_c = 3$, and $\Gamma = 0$.
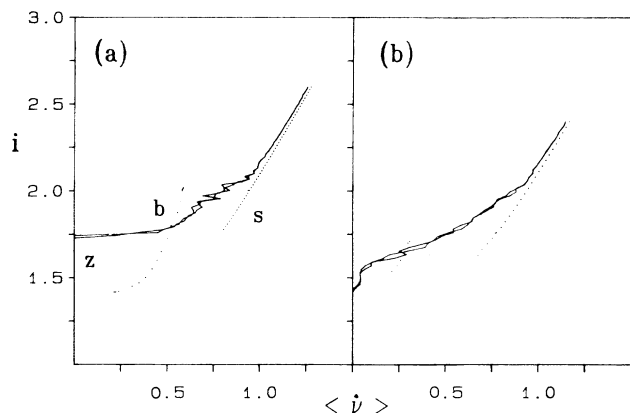
FIG. 4. i-$\langle \dot{v} \rangle$ characteristics (solid line) corresponding to (a) $\theta_{ext}=0$ and (b) $\theta_{ext}=1.57$ computed in the case $\beta_L=6.28$, $\beta_c=3$, and $\Gamma=0.01$ with an integration time step of 0.01 and total time $T=2621$. To facilitate the comparison the dotted lines represent the same characteristics as in Fig. 2 ($\Gamma=0$).

measurements on noise and sensitivity of planar gradiometers with integrated dc SQUID's,[6] which are characterized by values of β_L and β_c like those described here. In these devices the SQUID inductance itself is the magnetic field detector, the SQUID being designed in a second-order gradiometer configuration consisting of four loops connected in parallel. In this case, the sensitivity of such a device to the external magnetic field increases approximately with the square of the loop side, while the total SQUID inductance increases linearly with the side.

In the case of the single Josephson junction it has been shown[7] that the effect of noise is to cause occasional random switching between the "zero-voltage state" and the "voltage-different-from-zero state." This random switching leads to a large increase of the low-frequency voltage noise spectral density as well as the absence of hysteresis in the current-versus-voltage curve.

The noisy i-$\langle \dot{v} \rangle$ characteristics for the dc SQUID in the case $\beta_L=6.28$ and $\beta_c=3$ corresponding to $\theta_{ext}=0$ and 1.57 are shown in Fig. 4. Each characteristic is obtained by using 200 different points. The curve is obtained with the process described previously and $\Gamma=0.01$. The integration time step Δt of Eq. (2) is 0.01 for a total time $T=2621$. The noise currents i_{n1} and i_{n2} are simulated using a Gaussian-distributed random generator of $\sigma=(2\Gamma/\Delta t)^{1/2}$ to generate two independent sequences of current pulses (the duration of each pulse is Δt). Note the absence of hysteresis, the increasing-current branch being almost completely superimposed on the decreasing-current branch. In Fig. 5 $\dot{v}(t)$ and $J(t)$ corresponding to the point $i=1.9697$ and $\theta_{ext}=0$ of the above noisy i-$\langle \dot{v} \rangle$ characteristic are shown. Each point represented in Fig. 5 is the result of an average over 256 adjacent points. In this figure transitions between the single junction state and the beating state are visible. The single junction state is characterized by a higher average voltage and low circulating current pulses, whereas the beating state is characterized by lower average voltage and high circulating current pulses. It is evident that the noise causes occasional jumps
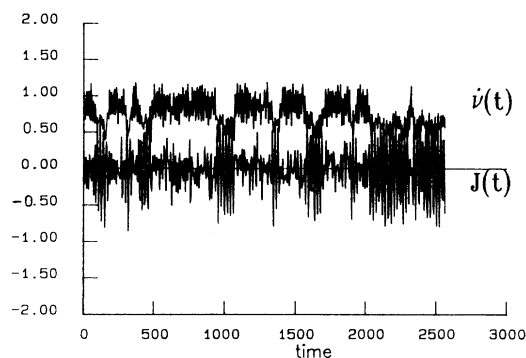
between the possible different branches. Here, the result is the destruction of the multiplicity of the states and the merging of the two branches into one average curve that, for a certain range of the current i, passes near the beating branch or near the single junction branch. It is interesting to point out that this hopping mechanism surely produces an increase of the low-frequency voltage noise level.

In Fig. 6 we show the voltage-versus-flux characteristics for $i=1.6$ and $i=1.8$, in the cases $\beta_L=6.28$, $\beta_c=3$, $\Gamma=0.01$, $\Delta t=0.01$, and $T=2621$. Two curves of 100 points are computed for each current value: They are generated starting from different noise current sequences and initial conditions. In order to be sure that the total time is long enough we repeated the computation for a few (24) points with a total time $T=41943$; the results are shown as full squares in Fig. 6. Note, for $i=1.6$, the disappearance of the curve portion corresponding approximately to $\theta_{ext}\leq 0.8$ and $\theta_{ext}\geq 5.5$ and, at the same time, the appearance of a portion of curve with responsivity $\partial\langle\dot{v}\rangle/\partial\theta_{ext}$ enough different from zero. It is possible to get this appre-
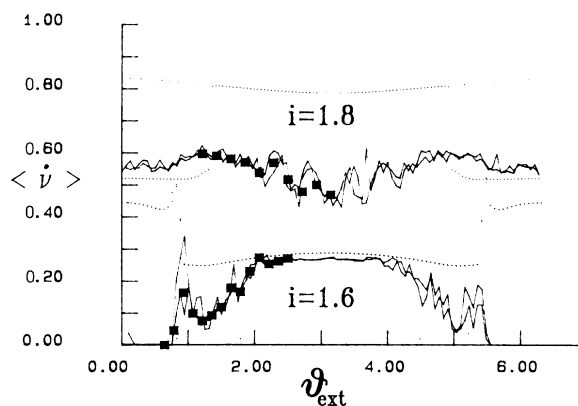

FIG. 5. $\dot{v}(t)$ and $J(t)$ solutions corresponding at the point $i=1.9697$ of the i-$\langle \dot{v} \rangle$ characteristic shown in Fig. 4(a).

FIG. 6. $\langle\dot{v}\rangle$-θ_{ext} characteristics corresponding to $i=1.6$ and $i=1.8$ in the case $\beta_L=6.28$, $\beta_c=3$, and $\Gamma=0.01$ computed with an integration time step of 0.01. The solid line is calculated using 200 points, each one averaged over a total time $T=2621$, the filled squares represent averages over $T=41943$. To facilitate the comparison the dotted lines represent the same characteristics shown in Fig. 3 ($\Gamma=0$).

ciable responsivity thanks to the hopping mechanism between the zero voltage branch and the beating branch. Considering only half a flux quantum (i.e., $\theta_{ext} \le \pi$) and looking at the solutions $v(t)$, it is possible to state that for $\theta_{ext} \le 0.8$ the system will be in zero voltage state. On the other hand, for $\theta_{ext} \ge 2$ it will be in the beating state. For intermediate θ_{ext}, random switching occurs between these two branches, and the total time during which the system is in one state or in the other depends approximately linearly on θ_{ext}. At $i = 1.8$ the random switching occurs between the beating state and the single junction state resulting in a less regular characteristic.

It is worthwhile to estimate the low-frequency flux sensitivity of such a device. The low-frequency noise flux spectral density is given by

$$S_\phi^0 = S_V^0 (\partial \phi_{ext}/\partial V)^2, \tag{7}$$

where S_V^0 is the voltage spectral density of V. Transforming into reduced units the right-hand side of Eq. (7) we get

$$S_\phi^0 = (\phi_0/2\pi)^4 (\Gamma/k_B T R) S_v(\partial v/\partial \theta_{ext})^{-2}. \tag{8}$$

For a temperature $T = 4.2$ K the flux sensitivity ϕ_N in ϕ_0 units is

$$\phi_N/\phi_0 = 6.89 \times 10^{-6} (\Gamma/R)^{1/2} S_v^{1/2} (\partial v/\partial \theta_{ext})^{-1}. \tag{9}$$

The voltage noise spectral density is evaluated at the point $i = 1.6$, $\theta_{ext} = 1.57$ of Fig. 6 with $\Gamma = 0.01$, applying the fast-Fourier-transform algorithm to 2^{14} points (each point is the average over 256 contiguous points) of the $v(t)$, computed for a total time $T = 41\,943$ and a time step $\Delta t = 0.01$. The voltage spectral density is flat for frequen-cies less than 0.001 and we estimate here $S_v = 4.5$. The calculated local responsivity around this working point is 0.15 and assuming $R = 15\,\Omega$ we obtain $\phi_N = 2.5 \times 10^{-6} \phi_0$ $Hz^{-1/2}$. This number is not too different from that reported in Ref. 6 of $8 \times 10^{-6} \phi_0$ $Hz^{-1/2}$ considering that, in that case, the dc SQUID was characterized by $R = 15\,\Omega$, $\beta_c = 2.2$, $\beta_L = 8.1$, and $\Gamma = 0.016$.

We can conclude that considering only the effect of noise in the simulation is possible to understand the working mechanism of SQUIDs with a high value of β_L and β_c and relatively small value of the noise parameter Γ. The simulated Johnson noise makes some solutions unstable and the hopping mechanism between different branches can eliminate the multiplicity of the characteristics and can give a responsivity no longer flat. The computer simulation agrees quite well with previously reported measurements on a device suitable for applications, such as an array of large size planar gradiometers,[8] where very high SQUID inductances and relatively high critical currents are needed. A flux noise of the order of a few $10^{-6} \phi_0$ $Hz^{-1/2}$, in a device without input coil, surely higher than the noise of the best dc SQUIDs, can provide devices with magnetic field sensitivity better than any other existing gradiometer. The effect of the input coil usually spoils the overall performances of the dc SQUID.[9] The experimental measurements on real device are in progress.

[1]C. D. Tesche and J. Clarke, J. Low Temp. Phys. **29**, 301 (1977).

[2]V. J. deWaal, P. Schrijner, and R. Llurba, J. Low Temp. Phys. **54**, 215 (1984).

[3]J. A. Ketoja, J. Kurkijarvi, and R. K. Ritala, Phys. Rev. B **30**, 3757 (1984).

[4]E. Ben-Jacob and Y. Imry, J. Appl. Phys. **52**, 6802 (1981).

[5]W. D. Milne, *Numerical Solutions of Differential Equations* (Dover, New York, 1970), p. 64.

[6]P. Carelli and V. Foglietti, J. Appl. Phys. **54**, 6065 (1983).

[7]R. F. Voss, J. Low Temp. Phys. **42**, 151 (1981).

[8]P. Carelli and R. Leoni, J. Appl. Phys. **59**, 645 (1986).

[9]P. Carelli and V. Foglietti, IEEE Trans. Magn. **MAG-21**, 424 (1984).